

ESTIMATION OF DATA MEMORY CAPACITY FOR CIRCULARLY POLARIZED SYNTHETIC APERTURE RADAR ONBOARD UNMANNED AERIAL VEHICLE PLATFORM (CP-SAR UAV)

P. Rizki Akbar^{1,2}, J.T. Sri Sumantyo¹, V.C.Koo¹ and H.Kuze¹

Abstract. Previously only linear polarization is widely used in the Synthetic Aperture Radar (SAR) system onboard spaceborne and airborne platforms. In such linearly polarized SAR (LP-SAR) systems, Faraday rotation in the ionosphere and platform posture will contribute to the system noise. Therefore to improve this situation, currently a novel Circularly Polarized Synthetic Aperture Radar (CP-SAR) sensor is developed in Microwave Remote Sensing Laboratory, Chiba University. Moreover, from this research, a new backscattering data based on circularly polarized wave in the remote sensing field can be obtained. As an early stage of the development of this CP-SAR sensor, we built an Unmanned Aerial Vehicle (UAV) platform for testing CP-SAR sensor capabilities. In this paper, we describe the novel CP-SAR sensor and the method to design CP-SAR UAV especially in estimating the requirement of data memory capacity. Also a smaller antenna is possible to be implemented since the 3-dB axial ratio on antenna characteristic becomes the main parameter in this new CP-SAR technique. Hence, a compact CP-SAR sensor onboard a small and low cost spaceborne platform yielding a high accuracy SAR image data can be realized in the near future.

Keywords synthetic aperture radar, circular polarization, 3-dB axial ratio, CP-SAR, unmanned aerial vehicle

1. Introduction

In the transmission and reception process, the microwave signal that used by the conventional linearly polarized SAR (LP-SAR) spaceborne system is very sensitive from Faraday rotation that exists in the ionosphere (Rignot, 2000). In the transmission process, the polarization plane orientation of the microwave signal that impinging the earth surface will be altered as compare to the signal that transmitted by the SAR sensor (Dubois-Fernandez et al., 2008; Wright et al., 2003). Here, this polarization plane orientation is defined as the tilt angle, τ (see Figure 2).

In the receiver part, the difference polarization plane orientation ($\Delta \tau$) between the implemented LP-SAR antenna receiver system and the reflected linear polarization wave could cause mismatch polarization loss in the receiver SAR system.

For the L-band frequency which is suitable for land observation and vegetation monitoring, in the worst case it is predicted that the value of Faraday rotation could achieve up to 40° (Freeman, 2003). Also from Meyer and Nicoll (2008) could be studied that the value exceeding 25° of Faraday rotation exists in the PALSAR sensor onboard Advance Land Observation Satellite-ALOS.

In the scattering process, since the polarization plane orientation of the signal resulted scattering mechanism will be different from time to time depends on the condition of the ionosphere. Thus, the usage of circularly polarized (CP) wave is expected to become a suitable solution for SAR spaceborne multitemporal observation (Dubois-Fernandez et al., 2008) as the signal plane orientation that arrives on the Earth surface will stay the

¹ Chiba University, Japan

² Multimedia University, Malaysia

same as the transmitted one. Although in other microwave systems, such as in the communication system (International Telecommunication Union, 2002) and the radio astronomy application (Raney, 2007), this circularly polarized wave has been commonly used, but its application in the spaceborne SAR for Earth observation has never been accomplished.

The major challenge in realizing this system is achieving adequate value of axial ratio (AR), S parameter, input impedance and gain simultaneously within the targeted bandwidth around the operational frequency on the implemented antenna system. Therefore, our Laboratory currently has been developing a novel SAR sensor based on the circularly polarized microwave (Rizki Akbar et al. 2010). In its development stages, firstly, the CP-SAR sensor will be tested onboard airborne platform, named as Josaphat Laboratory Experimental UAV (JX-1) (see Figure 1 that come toward to the Earth surface will be influenced by Faraday rotation, the and Table 1). The operating frequency is 1.27 GHz (L-band) and the Range Doppler Algorithm is used in the signal processing. From this CP-SAR UAV experiment, a remarkable knowledge for CP-SAR system onboard a small satellite (CP-SAR PSAT) realization is expected to be obtained. This CP-SAR PSAT is scheduled to be launched in the near future of 2014 (Sri Sumantyo et al. 2009).

Furthermore, a new kind of backscattering data in the field of remote sensing based on circular polarized microwave usage could be obtained by using our CP-SAR sensor. In the next section of this paper the microwave polarization classification based on the AR value will be discussed. Then, in section 3, the novel CP-SAR fundamental will be explained. Section 4 will describe the method to estimate the raw data memory capacity for CP-SAR UAV and the results.

Finally the summary will be given in section 5.

Table 1. Basic Specification of JX-1

Payload	25 kg
Endurance	4-6 hours
Altitude	1-4 km
Speed	100-120 kph

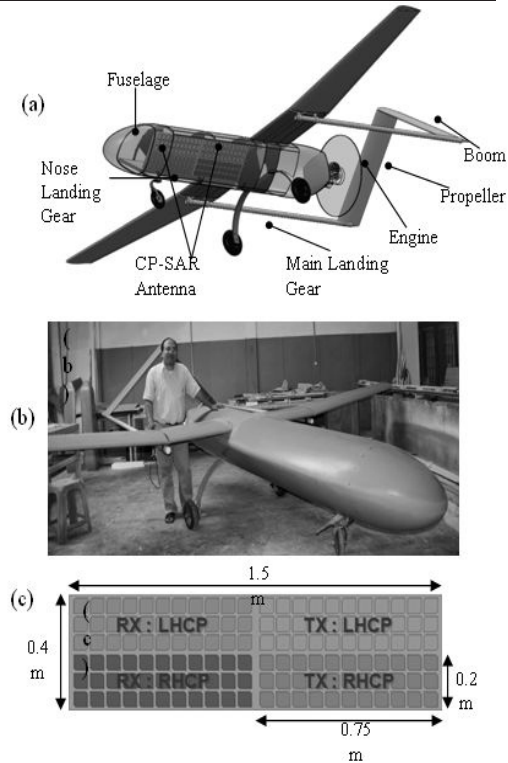


Figure 1. (a) describe the Josaphat Laboratory Experimental UAV (JX-1), (b) the photograph of JX-1 and (c) the CP-SAR antenna array configuration.

2. Axial Ratio (AR) in Polarization Classification

In the microwave system, the value of AR parameter (R) is used to determine the type of wave polarization. Here, R is defined as (Stutzman, 1993)

$$\varepsilon = \cot^{-1} (-R), \quad (1)$$

where ε represents the ellipticity angle ($-45^\circ \leq \varepsilon \leq 45^\circ$) (see Figure 2). Generally, there are three types of polarization, i.e. circular polarization, linear polarization and elliptical polarization. R is equal to 1

and infinite for circular polarization and linear polarization, respectively. In case of elliptical polarization, R is in between of 1 up to infinite. Practically, R is presented in dB unit as $20 \log_{10}|R|$. The absolute value of R then also can be estimated as the ratio of the maximum (OA) and minimum value (OB) of the electric field amplitude. In regards to polarization sense, the sign of R is positive for right-handed (RH) polarization and negative for left-handed polarization (LH).

In our CP-SAR UAV system (see Figure 3), the circularly polarized microwave is generated by feeding the CP-SAR antenna system in order that the radiated electromagnetic wave will have a 90° phase difference (δ) between y component (E_y) and x component (E_x). Here, the direct feeding method is used in our CP-SAR UAV system (Baharuddin et al., 2010; Yohandri et al., 2011). The value of G should be -90° and 90° to generate left-hand circular polarization (LHCP) and right-hand circular polarization (RHCP), respectively. Although, theoretically, for perfect circularly polarized wave the R value should be 0 dB, our experiment results (Baharuddin et al., 2010; Yohandri et al., 2011) have shown that practically this condition is very difficult to be achieved. Hence, in our CP-SAR system, both of our LHCP and RHCP antenna array radiation pattern characteristic are targeted to have AR less than 3-dB in their operational beamwidth, as explained in detail in section 3.

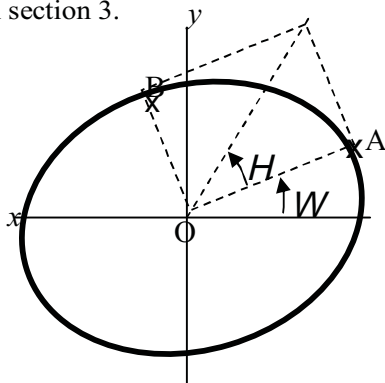


Figure 2. Electromagnetic Wave Polarization Parameters

3. Fundamental of CP-SAR System

In the conventional LP-SAR system, the effective footprint for both elevation and azimuth direction is determined by the 3-dB half power beamwidth of the antenna system. This 3-dB half power beamwidth is defined as the antenna beamwidth of gain, where the antenna still has gain up to 3-dB down in comparison with its maximum gain in the antenna main lobe radiation pattern (see Figure 4). This 3-dB half power beamwidth is related to the antenna physical size as (Stimson, 1998)

$$\theta_{el-LP} = 0.88 \frac{\lambda}{W},$$

$$\theta_{az-LP} = 0.88 \frac{\lambda}{L}, \quad (2)$$

where W , L and O is the physical antenna width, the physical antenna length and the operational radar wavelength, respectively. On the elevation direction, the value of θ_{el-LP} determines the swath width ground that could be covered by the LP-SAR system (Freeman et al., 2000). On the azimuth direction, the θ_{az-LP} is related to the synthetic aperture length (L_{sa-LP}) and the estimated azimuth resolution (δ_{az-LP}) as (Tomiyasu, 1978)

$$L_{sa-LP} = R_o \theta_{az-LP}, \quad (3)$$

$$\delta_{az-LP} = \frac{R_o \lambda}{2 L_{sa-LP}} \approx \frac{L}{2},$$

where R_o is the nearest range distance to the target in azimuth plane view as described in Figure 5 (b).

In the novel CP-SAR system, the effective footprint is determine by two antenna parameters which are the 3-dB half power beamwidth and the 3-dB AR beamwidth. The first parameter has already explained in Equation (2). The 3-dB AR beamwidth is defined as the antenna beamwidth within the 3-dB half power beamwidth which the antenna radiation pattern has R value up to 3-dB (see Figure 4). This 3 dB AR beamwidth is expressed as

$$\theta_{el-CP} \leq \theta_{el-LP}, \quad (4)$$

$$\theta_{az-CP} \leq \theta_{az-LP},$$

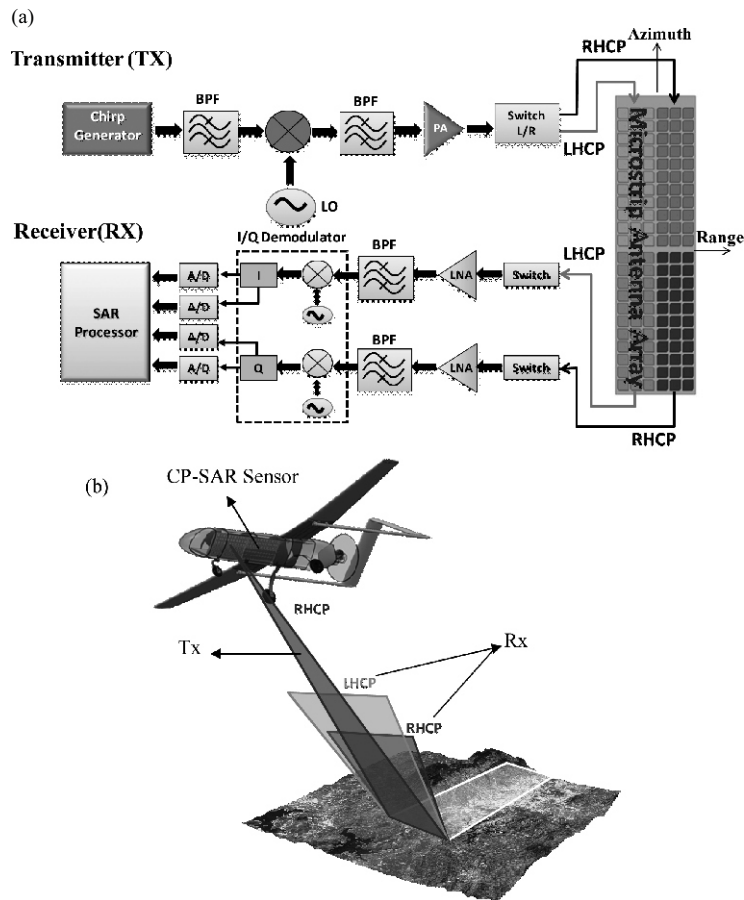


Figure 3. The CP-SAR UAV system: (a) CP-SAR UAV hardware configuration and (b) CP-SAR UAV in the operation mode. In (b), CP-SAR UAV is transmitting (Tx) RHCP signal and receiving (Rx) both the LHCP and RHCP signal simultaneously.

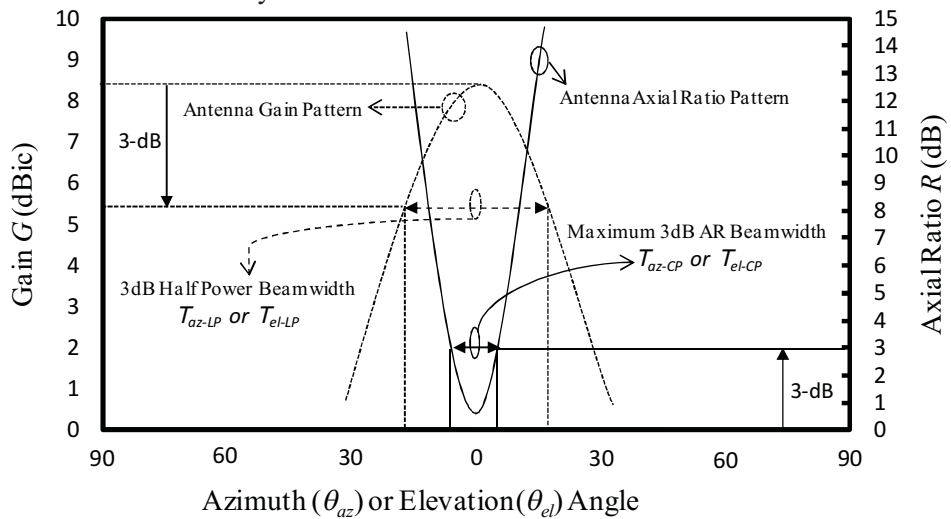


Figure 4. Main lobe radiation pattern of a single patch CP-SAR antenna.

4. Data Memory Capacity Estimation

4.1.CP-SAR UAV Geometry System

Base on explanation in section 3, the CP-SAR UAV geometry system can be derived as shown in Figure 5. Here, the far range and near range are determined by T_{el-CP} as

$$R_f = \frac{H}{\cos(\theta_o - (\theta_{el-CP} / 2))},$$

$$R_m = \frac{H}{\cos \theta_o},$$

$$R_n = \frac{H}{\cos(\theta_o + (\theta_{el-CP} / 2))},$$

where, R_f and R_n are the CP-SAR UAV far range and near range, respectively, H is the UAV platform altitude, and θ_o is off nadir angle. R_m is the CP-SAR middle slant range related to θ_o .

The incidence angle θ_i can be estimated using the following equation:

$$\theta_i = \sin^{-1} \left(\sin \theta_o \frac{R_e + H}{R_e} \right) \quad (8)$$

where R_e is the Earth radius (≈ 6371 km). For airborne system, the value of H is relative small compare to R_e ($H \ll R_e$) thus the result of $\theta_i | \theta_o$ will be obtained. The CP-SAR swath width ground (W_{g-CP}) can be estimated as follows

$$W_{g-CP} = \sqrt{R_f^2 - H^2} - \sqrt{R_n^2 - H^2}, \quad (9)$$

and substituting equation (5) and (7) into equation (9) yields

$$\sqrt{\left(\frac{1}{\cos(\theta_o + (\theta_{el-CP} / 2))} \right)^2 - 1} - \sqrt{\left(\frac{1}{\cos(\theta_o - \theta_{el-CP} / 2)} \right)^2 - 1} - \frac{W_g}{H} = 0 \quad (10)$$

In the azimuth direction, the synthetic aperture length of the CP-SAR UAV (L_{SA-CP}) and azimuth resolution (δ_{az-CP}) are determined by

$$L_{SA-CP} = R_o \theta_{az-CP}, \quad (11)$$

$$\delta_{az-CP} = \frac{R_o \lambda}{2L_{SA-CP}} = \frac{\lambda}{2T_{az-CP}}.$$

In the range direction, the ground range resolution (δ_g) can be estimated as (Cumming and Wong, 2005)

$$\delta_{gr} = \frac{c}{2B \sin \theta_i}, \quad (12)$$

where c is the velocity of light (3×10^8 ms⁻¹) and B is the chirp pulse bandwidth. From Figure 6, the total length of flight (L) that should be covered by the CP-SAR UAV to take data for the targeted image size (I_{CP}) can be expressed as

$$L = L_o + L_{SA-CP}, \quad (13)$$

where L_o is the length of the image size that targeted to be covered and the parameter L_{SA-CP} is described in equation (11).

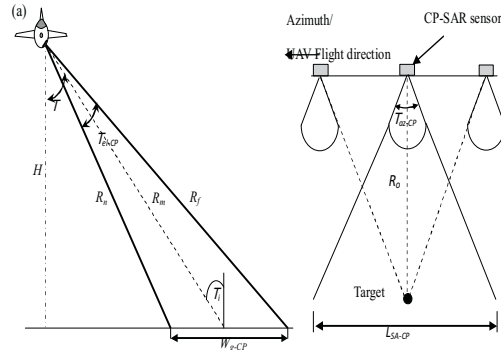


Figure 5. CP-SAR UAV geometry: (a) slant range plane and (b) azimuth plane

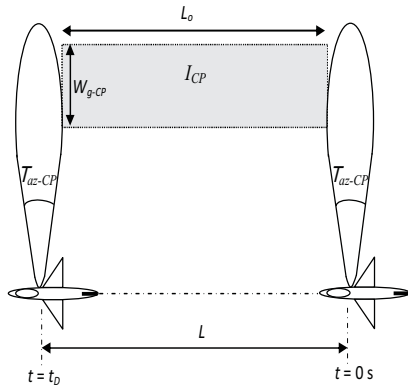


Figure 6. CP-SAR UAV data take process

4.1 CP-SAR Signal Processing Parameters

Figure 5 visualizes that in its 3-dB AR beamwidth coverage (both θ_{el-CP} and θ_{az-CP}), the SAR sensor receive the scattered pulses while it moves along the azimuth track. The nearest distance travelled by the scattered pulse to reach back the CP-SAR sensor is R_n . On the other hand, the farthest distance for the pulse to travel back to the sensor equals to the range maximum (R_{max}). This R_{max} is defined as the hypotenuse of the R_f and L_{SA-CP} and can be expressed as

$$R_{max} = \sqrt{R_f^2 + \left(\frac{L_{SA-CP}}{2}\right)^2}.$$

Both of these distance parameters, R_n and R_{max} , is the important parameters for controlling the starting time and stopping time in the SAR signal processor sampling process.

The start sampling time (t_{start}) is the time when CP-SAR system firstly begins to detect the reflected signal. This t_{start} parameter is defined as

$$t_{start} = \frac{2R_n}{c}, \quad (15)$$

where R_n is defined in Equation (5). The stop sampling time (t_{stop}) is described as

$$(16) \quad t_{stop} = \frac{2R_{max}}{c} + \tau_p,$$

where τ_p is the pulse length. Since in the airborne SAR system the reflected pulse will be received immediately by the sensor after a pulse transmission, the value of t_{start} parameter will limit the τ_p value. This situation is illustrated in Figure 7. Here, the length of transmitted pulse τ_p should be defined hence it would not collide with the receiving window. Therefore in our design, we set the switching time τ_{sw} as the period of time where the CP-SAR sensor changing its mode from transmitting pulse mode into the receiving mode. Here, τ_{sw} equals to $3 \mu s$ is defined. The value of τ_p also has to meet time bandwidth product (TBP) bigger than 100 requirement (Henderson and Lewis, 1998). Therefore, to determine the value of τ_p we can use the following formulas:

$$\tau_p = t_{start} - \tau_{sw},$$

$$\tau_p B > 100.$$

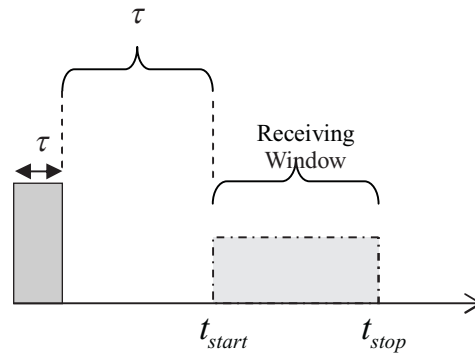


Figure 7. CP-SAR Pulse Timing Diagram.

The scattered signal will be received and processed during the receiving window interval. As illustrated in Figure 7, the receiving window interval (or time sampling interval) can be estimated from the difference between t_{start} and t_{stop} as

$$T_{si} = t_{stop} - t_{start}, \quad (19)$$

where T_{si} is the sampling time interval, t_{start} and t_{stop} defined in Equation (15) and (16).

4.2.a. Signal Processing in The Range Direction

Figure 8 shows the block configuration of general SAR processor (Koo et al., 2007). Here, the received signal (RF receiver output) is then sampled by using sampling frequency (f_s) which follows the Nyquist theorem. For our CP-SAR UAV system (Figure 3 (a)) that use complex I-Q signal format, the required f_s is (Cumming and Wong, 2005):

$$f_s = \alpha B, \quad (20)$$

where α is typically equal to 1.2. The spacing of each sample (Δt) can be expressed in time domain as the inverse of sampling frequency:

$$\Delta t = 1/f_s. \quad (21)$$

Hence in range direction, the number of samples per pulse (n) can be described as

$$n = T_{si} / \Delta t. \quad (22)$$

4.2.b. Signal Processing in The Azimuth Direction

The number of transmitted pulses that transmitted by the CP-SAR system during one second while it flies along the azimuth direction are defined as Pulse Repetition Frequency (PRF). Then we can formulate the sample spacing in aperture domain (Δs_{az}) as the sample spacing in aperture domain (Δs_{az}) as

$$\Delta s_{az} = \frac{v}{PRF}, \quad (23)$$

which Δs_{az} is in distance unit and v is the UAV velocity. The down sampling rate (K_p) in the SAR processor system can be estimated as

$$K_p \leq \frac{PRF}{1.2B_D}, \quad (24)$$

where B_D is the Doppler bandwidth which for the CP-SAR system can be estimated as (Rizki Akbar et al., 2010)

$$B_D = \frac{2vT_{az-CP}}{\lambda}, \quad (25)$$

which Δs_{az} is in distance unit and v is the UAV velocity. The down sampling rate (K_p) in the SAR processor system can be estimated as

$$K_p \leq \frac{PRF}{1.2B_D}, \quad (24)$$

where B_D is the Doppler bandwidth which for the CP-SAR system can be estimated as (Rizki Akbar et al., 2010).

$$B_D = \frac{2vT_{az-CP}}{\lambda}, \quad (25)$$

In our CP-SAR design, the maximum value of K_p in Equation (24) is used. Multiplying the value of K_p with Equation (23) resulting the azimuth sample spacing after presummer filter (du) as

$$du = K_p \Delta s_{az}. \quad (26)$$

Therefore, the number of samples on the azimuth aperture with length L can be written as

$$m = L/du \quad (27)$$

In order to obtain two dimensional SAR image of I_{CP} ($L_o \times W_{g-CP}$) data as shown in Figure 6, the required data memory capacity MC_D per channel

$$MC_D = n_b \times n \times m; \quad (28)$$

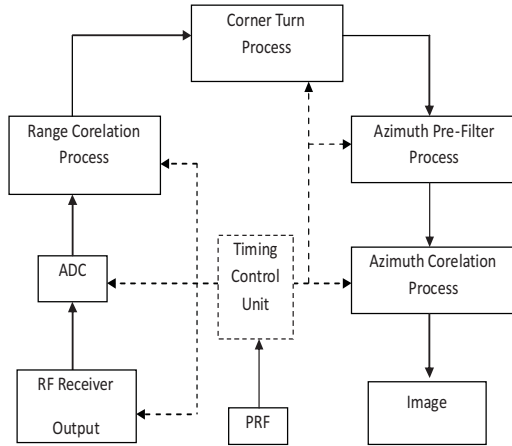


Figure 8. General SAR Processor Configuration

4.3 The Required MC_D and The Data Rate

In our CP-SAR UAV system, it is defined that

$$\delta_{gr} = \frac{W_{g-CP}}{1000}, \quad (29)$$

$$\delta_{az-CP} = \delta_{gr},$$

where δ_{az-CP} , δ_{gr} and W_{g-CP} is explained in equation (11),(12) and (9). Here, in our experiment, 1 km in W_{g-CP} , 1 m in δ_{az-CP} , 1000 cells in the ground range and 50 km² in I_{CP} are targeted. The angle between 40q up to 60° is chosen for our θ_o since the backscattering coefficient of nature targets such as soil, grass and vegetable are

maintained almost constant over these angles (Chan et al., 2007). By applying Equation (2), (4), (10), (11) and (29), the required θ_{el-CP} and θ_{az-CP} is estimated. Table 2 shows the required θ_{el-CP} with the 1° interval in θ_o . The value of 6.77° in θ_{az-CP} is obtained for all θ_o from 40q up to 60°. From here can be noticed that a smaller physical size of antenna can be use in the CP-SAR system, as long as the targeted θ_{el-CP} and θ_{az-CP} is achieved and still meet the equation (4) requirement. Consequently, a novel light and small CP-SAR sensor can be developed then a low-cost CP-SAR sensor onboard a small satellite can be realized.

Figure 9 (a) shows us the required ADC f_s by applying Equation (12), (18), (20) and (29). Here, can be seen that lower f_s is used for higher θ_o . The values of τ_p that applicable in our CP-SAR system are illustrated in Figure 9 (b). Longer τ_p can be used for higher θ_o and H since longer R_n (t_{start}) will be obtained. Figure 10 (a) describes the estimation of data memory capacity (MC_D) for 4 channel CP-SAR system with n_b is equal to 8 by applying Equation (13), (19), (21), (22), (26) and (27). In total, it is estimated 21.7 Gbits memory is required in our CP-SAR UAV system that flies up to 4 km in altitude. The required time for taking I_{CP} image data (t_D) can be calculated as

$$t_D = \frac{L}{v}, \quad (30)$$

where L is defined in (13). Then, the data rate per channel (DR) can be estimated as

$$DR = \frac{MC_D}{t_D}. \quad (31)$$

Figure 10 (b) illustrates the DR with t_D is 31 s for 4 channel CP-SAR system. The summary of our CP-SAR UAV parameters are shown in Table 3.

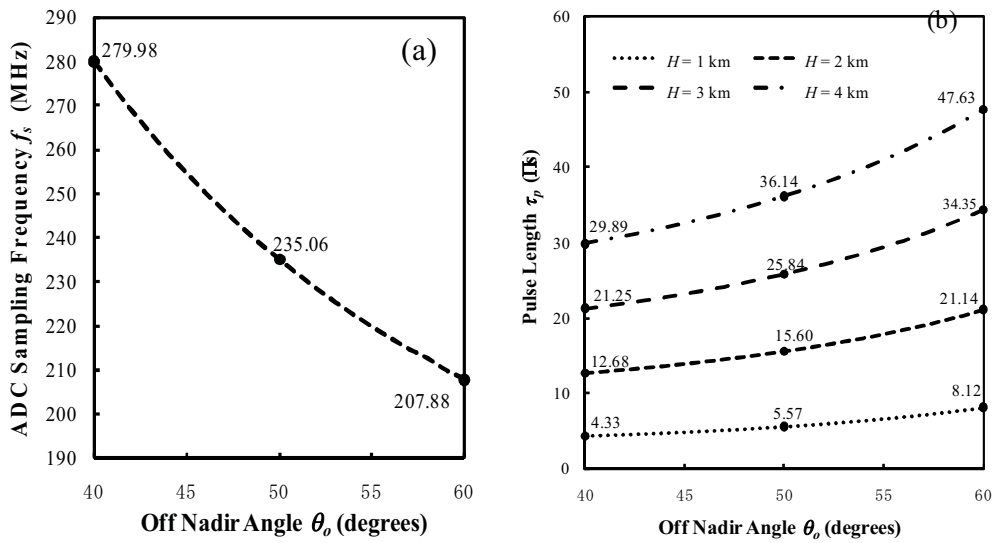


Figure 9. (a) The required f_s for 1m resolution and (b) the applicable τ_p .

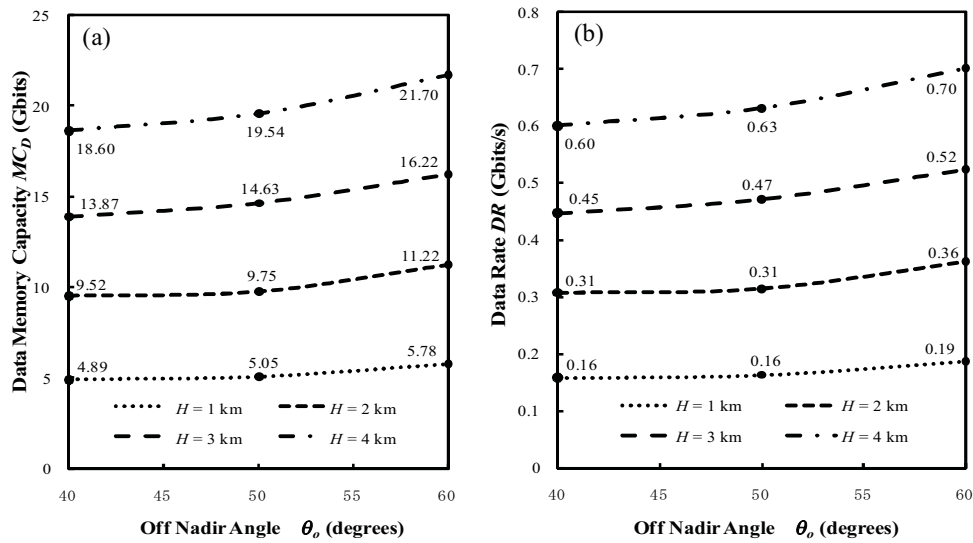


Figure 10. (a) the data memory capacity and (b) the data rate for 4 CP-SAR channels.

Table 2. List of the required θ_{el-CP}

θ_o (in degrees)	θ_{el-CP} (in degrees)				θ_o (in degrees)	θ_{el-CP} (in degrees)			
	1 km	2 km	3 km	4 km		1 km	2 km	3 km	4 km
40	31.02	16.45	11.1	8.36	51	21.23	11.15	7.5	5.65
41	30.13	15.97	10.77	8.11	52	20.35	10.67	7.18	5.41
42	29.24	15.49	10.45	7.87	53	19.48	10.2	6.87	5.17
43	28.35	15	10.12	7.62	54	18.62	9.74	6.55	4.93
44	27.46	14.52	9.79	7.37	55	17.77	9.28	6.24	4.69
45	26.57	14.03	9.46	7.13	56	16.92	8.82	5.93	4.46
46	25.67	13.55	9.13	6.88	57	16.08	8.37	5.63	4.23
47	24.78	13.07	8.8	6.63	58	15.26	7.93	5.33	4
48	23.89	12.58	8.48	6.38	59	14.45	7.5	5.04	3.79
49	23	12.1	8.15	6.14	60	13.64	7.07	4.75	3.57
50	22.11	11.62	7.82	5.89					

Table 3. CP –SAR UAV Specification

Parameter	Specification
Altitude	1 – 4 km
Frequency	1.27 GHz (L-Band)
Polarization	Tx : RHCP + LHCP Rx : RHCP + LHCP
Image Size	50 km ²
Pulse Length	4.33 up to 47.63 μ s
Pulse Bandwidth	173.23 up to 233.31 MHz
Off Nadir	40° up to 60°
Resolution	1m
Swadth width	1 km
Antenna Size	1.5 m x 0.4 m (0.75 m x 0.2 m each sub panel)
	6.77°
Azimuth Beamwidth	3.57°-31.02°
Elevation Beamwidth	≤3 dB
Axial Ratio	14.32 dBic
Antenna Gain	80%
Antenna Efficiency	1000 Hz
PRF	16.18 W up to 338.16 W
Peak Power	69.98 mW up to 16.11 W
Average Power	
System :	
Noise Figure	3 dB
Temperature	500 K
Loses System	3 dB
Switching Time	3 μ s
SNR	20 dB
Data Take Duration	31 minutes

5. Conclusion

In this paper, the fundamental of novel CP-SAR system has already explained. In the range of its 3-dB half power beamwidth, the CP-SAR antenna radiation pattern should also has Axial Ratio (AR) d 3-dB in both elevation and azimuth direction (θ_{el-CP} and θ_{az-CP}). The θ_{el-CP} and θ_{az-CP} determine all CP-SAR geometry system and signal processing parameters. Furthermore, as explained in section 4, based on the required value of θ_{el-CP} and θ_{az-CP} we can estimate the data memory capacity in the CP-SAR UAV application. Hence both θ_{el-CP} and θ_{az-CP} are become the main constraint in the hardware and parameter design. The implementation of a light and small sensor in the CP-SAR system becomes possible by this 3-dB AR dependency. Moreover, this CP-SAR UAV research will become a remarkable point to the CP-SAR sensor onboard a small satellite realization in the future.

Acknowledgements

The authors would like to thank the Japan Society for the Promotion of Science (JSPS) for Grant-in-Aid for Scientific Research 2007-Young Scientist (A) (No. 19686025), National Institute of Information and Communication Technology (NICT) for International Research Collaboration Research Grant, and Chiba University COE Startup Program-Small Satellite Institute for Earth Diagnosis FY 2009-2010.

References

Baharuddin, M., Rizki Akbar, P., Tetuko S.S, J., and Kuze, H., 2010, Development of circularly polarized synthetic aperture radar sensor mounted on unmanned aerial vehicle. *Jurnal Otomasi, Kontrol & Instrumentasi (Journal of Automation, Control and Instrumentation)*, 1:1-6.

- Chan, Y.K., Koo, V.C. and Lim, T.S., 2007, Conceptual Design of A High Resolution, Low Cost X-Band Airborne Synthetic Aperture Radar System. *Progress in Electromagnetic Research*, 3: 943-947.
- Cumming, I.G. and Wong, F.H, 2005, *Digital Processing of Synthetic Aperture Radar Data*. Artech House, USA.
- Dubois-Fernandez, P.C., Souyris, J.-C., Angelliaume, S. and Garestier, F., 2008, The compact polarimetry alternative for spaceborne SAR at low frequency. *IEEE Transactions on Geoscience Remote Sensing*, 46:3208-3222.
- Freeman, A., Johnson, W.T.K., Huneycutt, B., Jordan, R., Hensley, S., Siqueira, P., and Curlander, J. 2000. The "myth" of the minimum SAR antenna area constraint. *IEEE Transactions on Geoscience and Remote Sensing*, Vol. 38, No. 1 pp. 320-324.
- Freeman, A, 2003, Faraday Rotation and Interferometric/Polarimetric SAR. *ASAR Workshop*. Reterived 15 February 2011, from <http://trs-new.jpl.nasa.gov/dspace/bitstream/2014/7609/1/03-1625.pdf>
- Henderson, F.M. and Lewis, A.J., 1998, *Principles & Applications of Imaging Radar : Manual of Remote Sensing, Third edition, Volume 2*. John Willey & Son, Inc, USA.
- International Telecommunication Union, 2002, *Handbook on Satellite Communications, Third Edition*. Wiley-Interscience, USA.
- Koo, V.C., Chan, Y.K., Lim, T.S., 2007, A Real-time Hybrid Correlator for Synthetic Aperture Radar Signal Processing, *Proceedings of the Progress in Electromagnetics Research Symposium (PIERS- 2007)*, 26-30 March 2007, Beijing, China. pp. 1709 – 1712.
- Meyer, F.J. and Nicoll, J.B., 2008, Prediction, detection, and correction of Faraday rotation in full-polarimetric L-

- band SAR data. *IEEE Transactions on Geoscience Remote Sensing*, 46:3076-3086.
- Raney, R.K. 2007. Hybrid-polarity SAR architecture. *IEEE Transactions on Geoscience and Remote Sensing*, 45: 3397-3404.
- Rignot, E.J.M., 2000, Effect of Faraday rotation on L-band interferometric and polarimetric synthetic-aperture radar data. *IEEE Transactions on Geoscience Remote Sensing*, 38:383-390.
- Rizki Akbar, P., Sri Sumantyo, J.T., Kuze, H. 2010. A novel circularly polarized synthetic aperture radar (CP-SAR) onboard spaceborne platform. *International Journal of Remote Sensing*, Vol. 31, No. 4, pp. 1053-1060.
- Sri Sumantyo, J.T., Wakabayashi, H., Iwasaki, A., Takahashi, F., Ohmae, H., Watanabe, H., Tateishi, R., Nishio, F., Baharuddin, M., and Rizki Akbar, P, 2009, Development of circularly polarized synthetic aperture radar onboard microsatellite. *Proceedings of the Progress in Electromagnetics Research Symposium (PIERS- 2009)*, 23-27 March 2009, Beijing, China. pp. 382 – 385.
- Stimson, G.W, 1998, *Introduction to Airborne Radar, Second Edition*. SciTech Publishing Inc., USA.
- Stutzman, W.L, 1993, *Polarization in Electromagnetic System*. Artech House, USA.
- Tomiyasu, K, 1978, Tutorial review of Synthetic-Aperture Radar (SAR) with applications to imaging of the ocean surface. *Proceedings of the IEEE*, May 1978, 66:563-583.
- Wright, P.A., Quegan, S., Wheadon, N.S., Hall, C.D, 2003, Faraday rotation effects on L-band spaceborne SAR data. *IEEE Transactions on Geoscience Remote Sensing*, 41:2735-2744.
- Yohandri, Wissan, V., Firmansyah, I., Rizki Akbar, P., Sri Sumantyo, J. T., and Kuze, H., 2011, Development of circularly polarized array antenna for synthetic aperture radar sensor installed on UAV. *Journal of Progress In Electromagnetic Research C*, 19: 119-133.